J Electr Eng Technol Vol. 7, No. 6: 983-989, 2012
http://dx.doi.org/10.5370/JEET.2012.7.6.983

ISSN(Print) 1975-0102
ISSN(Online) 2093-7423

Effect of Oxygen for Diamond Film Synthesis with C-Hexane in Microwave Plasma Enhanced CVD Process

Sang-Bo Han†

Abstract – The purpose of this paper is to decide the optimum synthesis conditions of polycrystalline diamond films according to the ratio of gas mixture. Diamond films were deposited with cyclo-hexane as a carbon precursor by the microwave plasma enhanced chemical vapor deposition process. The optimum oxygen ratio to cyclo-hexane was reached about 125 % under the fixed 0.3% c-hexane in hydrogen. Oxygen plays a role in etching the graphitic components of carbon sp2 bond effectively. By OES measurement, the best synthesis conditions found out about 12.5 % and 15.75 %, which is the emission intensity ratios of CH(B-X) and Hβ on Hα, respectively. Also, the electron temperature was similar about 5,000 to 5,200 K in this work.

Keywords: Chemical vapor deposition, Cyclo-hexane, Diamond films, Electron temperature, Optical emission spectroscopy, Oxygen

1. Introduction

Diamond, diamond-like carbon (DLC), and carbon nanotube have large application fields. Among them, diamond has an excellent mechanical and electronic properties such as high thermal conductivity, the mechanical hardness and fracture strength, high carrier mobility, high strength of electric breakdown, the wide bandgap of 5.45 eV, and so on. Thus, diamond is currently one of the most promising materials for the useful application into the electronic and optoelectronic fields such as high temperature and high power devices, bio-sensors, mechanical parts, and so on [1-12].

Recently, much research has been carried out for synthesizing the high quality diamond thin-films using microwave plasma enhanced chemical vapor deposition (MWPCVD) [13-17], radio frequency (RF), DC plasma CVD [18, 19], electron cyclotron resonance (ECR) plasma CVD [20-22], the hot filament CVD [23, 24], the ion beam deposition method (IBD) [25], laser ablation, combustion flame, etc [26-28]. Generally, the low pressure CVD processes for synthesis of diamond films have been used with the activating gas phase carbon-containing precursor of CH_4.

In this paper, polycrystalline diamond film was synthesized with cyclo-hexane (c-hexane, C_6H_{12}) instead of CH_4 as a carbon precursor in the low pressure MWPCVD process.

A. Grigonis et al. [25] reported the influence of hydrogen contents on the deposition of amorphous hydrogenated carbon films with hexane and acetylene. In addition, *M. Asmann et. al* [29] explained that the quality of diamond films increased by etching graphitic components from Cl, F and HF. However, the effect of oxygen has not been discussed, and their synthesis processes were completely different with this work. Furthermore, the analysis of the optical emission spectroscopy (OES) measurement have not directly compared with the quality of the synthesized diamond films.

Therefore, effects of oxygen and c-hexane contents related with the quality of diamond films carried out in comparison with results of OES measurement.

2. Experimental details

Diamond films were fabricated with c-hexane as a carbon precursor with hydrogen background gas by the 2.45 GHz MWPCVD process. Plasma was generated inside the quartz tube, which is 50 mm in outer diameter and 400 mm in height, and the microwave power was maintained at 700 W.

A Si (100) wafer substrate (10 mm by 10 mm in size) was pretreated to facilitate the diamond nucleation by a supersonic treatment with diamond pastes of 1 μm in methanol solution, and cleaned with acetone, methanol, and distilled water subsequently. It was placed on the Si_3N_4 sample holer at the inside of plasma reactor. The pressure and hydrogen flow rate were fixed at 40 Torr and 60 sccm, respectively.

Gas phase c-hexane was supplied by a mass flow controller, it was evaporated from liquid in the canister. Temperature of the canister was controlled at 10 ℃ to prevent the phase change into liquid on the flow line under room temperature. The whole growth was performed for 4 hours and the synthesized films were characterized by raman shift spectra, scanning electron microscopy (SEM), X-ray photoelectron spectroscopy (XPS).

Raman shift spectra (System 2000, Renishaw) is measured with an Ar laser (514.5 nm), and SEM (CX-100SM) is

† Corresponding author: Dept. of Electrical Engineering, Kyungnam University, Korea. (hansangbo@kyungnam.ac.kr)
Received: May 10, 2012; Accepted: August 21, 2012

used to investigate the surface morphology and the thickness of films. In the XPS (Escalab 250, VG Scientifics) analysis, the energy source is the monochromatic Al-K$_\alpha$ of 1486.6 eV with the high resolution of 0.45 eV. Prior to analysis, the surface of samples is etched for 20 seconds to remove absorbed species by an Ar etching source.

Additionally, OES measurement was carried out by changing flow rates of c-hexane and oxygen. Total emission was measured by the optical fiber, and the acquired light was transmitted to the entrance slit of the monochromator (Spectrapro 2300i, slit: 20 μm). The final detection was done with a multichannel charged coupled device (CCD, temp.:-40 ℃).

Emission intensities of H$_\alpha$ (656.4 nm), H$_\beta$ (486.3 nm) and CH (B-X, 388.9 nm) were analyzed. The electron temperature was calculated using the relative intensity ratio of hydrogen atomic lines as follows [30],

$$T_e(K) = \frac{hc}{k} \times (E_\alpha - E_\beta) \times \left[\ln \left(\frac{I_\beta}{I_\alpha} \times \frac{\nu_\alpha \times A_\alpha \times g_\alpha}{\nu_\beta \times A_\beta \times g_\beta} \right) \right]^{-1} \quad (1)$$

Where,

α, β : the subscript for emissions of H_α and H_β;
h : the plank's constant (4.135×10^{15} eV·s);
c : the velocity of light (3×10^{10} cm/s);
k : the boltzmann constant (= 8.617×10^{-5} eV/K);
I : the intensity (arb. units);
A : the transition probability ($\times 10^7\ s^{-1}$);
E : the energy (cm^{-1});
ν : transition frequency (cm^{-1});
g : the statistical weight, it depends on the quantum numbers of the upper level (g=2J+1).

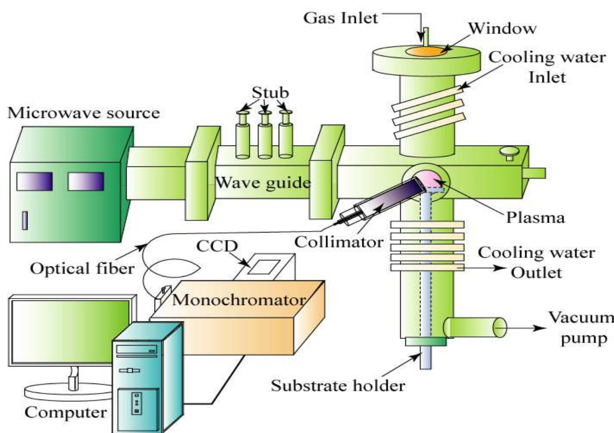

Fig. 1. Schematics of MWPCVD process.

Table 1. Constants for the calculation of the electron temperature

	λ (nm)	ν (cm^{-1})	E (cm^{-1})	g	A ($\times 10^7$ (s^{-1}))
H$_\alpha$	656.285	15237.3	97492.36	6	6.465
H$_\beta$	486.136	20570.4	102823.89	6	2.062

3. Results and Discussions

Table 2 shows the identification of synthesized samples according to experimental conditions. The first three samples are fabricated with mixtures of hydrogen and c-hexane without oxygen. The next four samples are synthesized to investigate the influence of oxygen. The last three samples is to investigate the optimum oxygen to c-hexane amounts under the constant 0.3 % c-hexane in hydrogen

Table 2. Identification of synthesized samples

Sample	c-hexane/H_2 (%)	O_2/H_2 (%)	O_2/c-hexane (%)
DS1	0.3	-	-
DS2	0.7		
DS3	1.3		
DS4	0.3	0.3	
DS5	0.7		
DS6	1.3		
DS7	2.0		
DS8	0.3	0.4	125.0
DS9		0.6	175.0
DS10		0.8	225.0

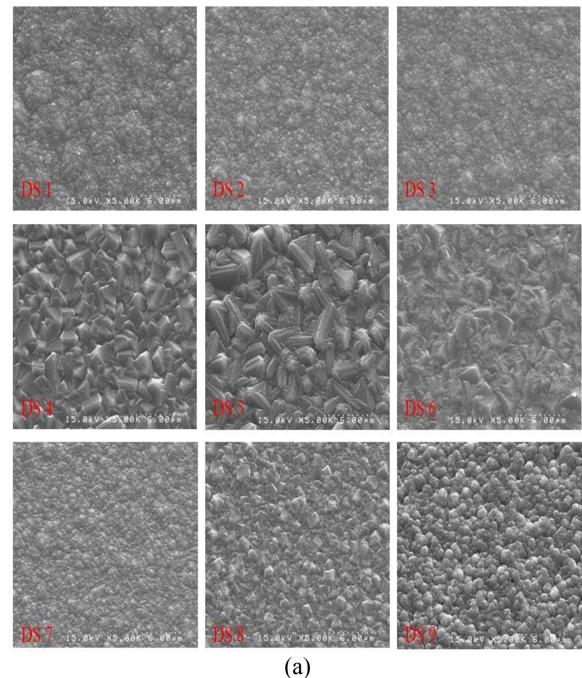

(a)

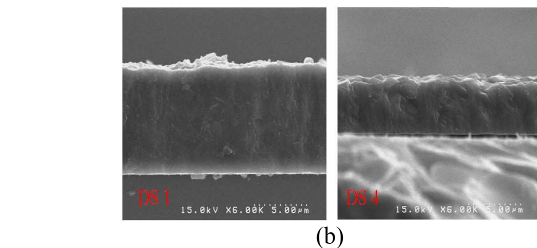

(b)

Fig. 2. Results of SEM measurement: (a) Surface morphology; (b) Cross-sectional views of films.

3.1 Effects of oxygen and c-hexane contents

Fig. 2 shows the surface morphology and cross-sectional views of synthesized films by SEM measurement. DS1, DS2, and DS3 samples are mainly composed of graphitic components, and DS4 and DS8 samples look like polycrystalline diamond films. Furthermore, the DS5 sample seems to be mixed diamond and graphitic components, the DS9 sample is laregely changed into the rounded grain boundary. The DS10 sample was not synthezied into films, therefore, it is not depicted in Fig. 2(a).

In Fig. 2(b), thickness of DS1 and DS4 samples are approximately 7.8 and 3.7 μm, respectively. Each growth rate corresponds to 1.95 μmh^{-1} and 0.92 μmh^{-1}, respectively. This implies that the the growth rate is largely affected by oxygen amounts.

In analysis of raman spectra, the peak at 1335 cm^{-1} can be assigned to the carbon sp^3 bond (D band) and the peak at 1580 cm^{-1} corresponds to the carbon sp^2 graphitic bond (G band) [25]. And the peak near 1140 cm^{-1} is popular known as the nanocrystalline diamond (NCD) [31].

The ratio of the intensity of the D and the G band is closely related with the carbon bonding ratio of sp^3 and sp^2 in films. Although the intensity of the G band is similar to that of the D band, this does not mean that the sp^2 bonded carbon is dominant in the film, because the cross-section of raman scattering around the G band is about 50~60 times higher than that of D band [32-35].

In Fig. 3(a), intensity of the D band was very weak, but that of G band were so strong. The presence of a weak peak near 1140 cm^{-1} indicates the evidence of NCD as well. From these results those films were mainly composed of graphite with a little NCD as explained in Fig. 2(a).

Therefore, it is necessary for the effective etching of sp^2 bond to improve the quality of diamond film. Intensity of D band increased largely by adding oxygen in Fig. 3(b) in comparison with Fig. 3(a) as the same ratio of c-hexane and hydrogen. However, the intensity of the D band decreased by increasing c-hexane amounts in hydrogen, it might be ascribed that the supplied oxygen for etching sp^2 graphitic bond was not sufficient. Thus, the effect of oxygen was investigated additionally under the fixed 0.3% c-hexane in hydrogen as in Fig. 3(c). The intensity of the D band in the DS8 sample was better than that in the DS4 sample, and the G band decreased a little as well. This result agrees with the result of Fig. 4(b).

In the case of the DS9 sample, both D band and G band were removed simultaneously, and it seems to be changed into DLC. Also, the DS10 sample was not synthesized into film by the excessive supplement of oxygen.

Intensity ratios of D and G bands were depicted in details as in Fig. 4. Intensities of the D band in DS4 and DS5 samples are so strong compared to that of DS1 and DS2 samples, and it decreased with increasing c-hexane amounts like in the DS6 and DS7 samples. Thus, the DS8 sample is the best diamond film in this experiment.

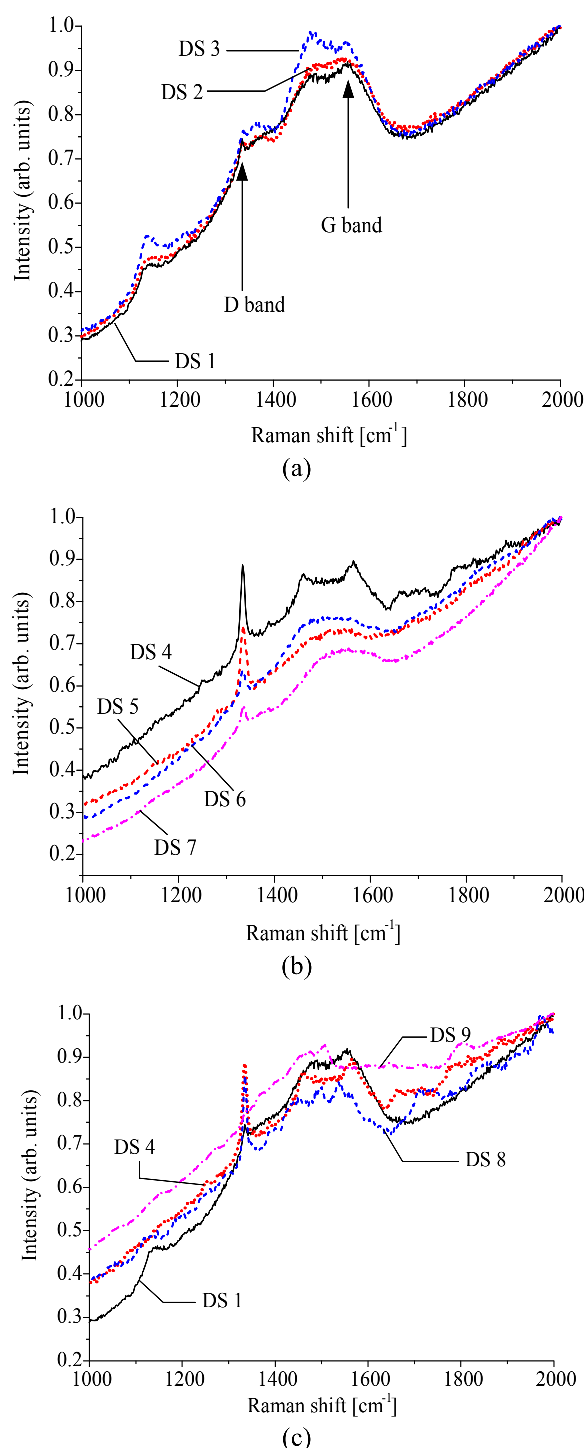

Fig. 3. Results of raman shift spectra: (a) Effect of c-hexane content; (b) Effects of oxygen content; (c) Both effects of oxygen and c-hexane contents.

For the effective synthesis of diamond films, the best oxygen amounts to c-hexane was reached about 125 %, which corresponds 0.4% oxygen amounts in hydrogen as depicted in Fig. 4(b).

Consequently, the synthesis of high quality diamond films is necessary to control the supplied oxygen amounts

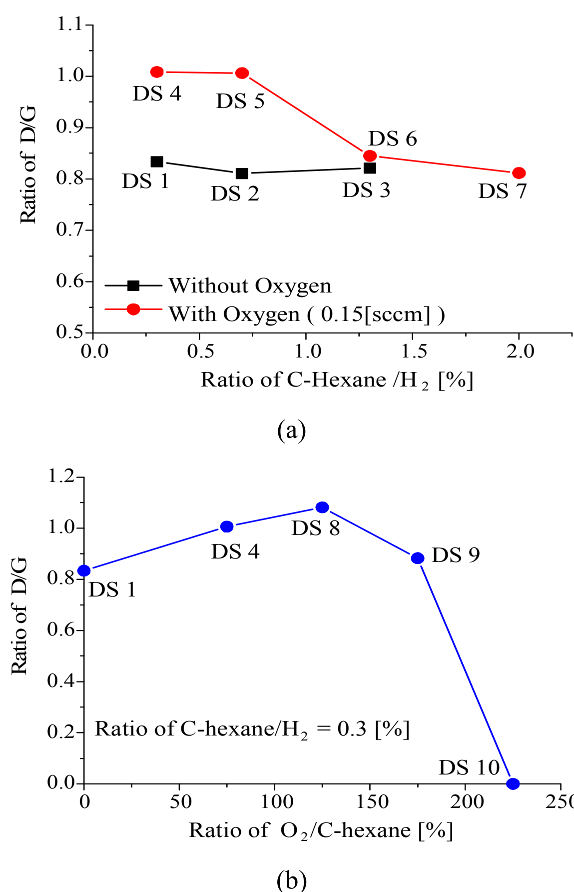

Fig. 4. The comparison of D band and G band according to the ratio of gas mixture: (a) On the ratio of c-hexane to hydrogen; (b) On the ratio of oxygen to c-hexane.

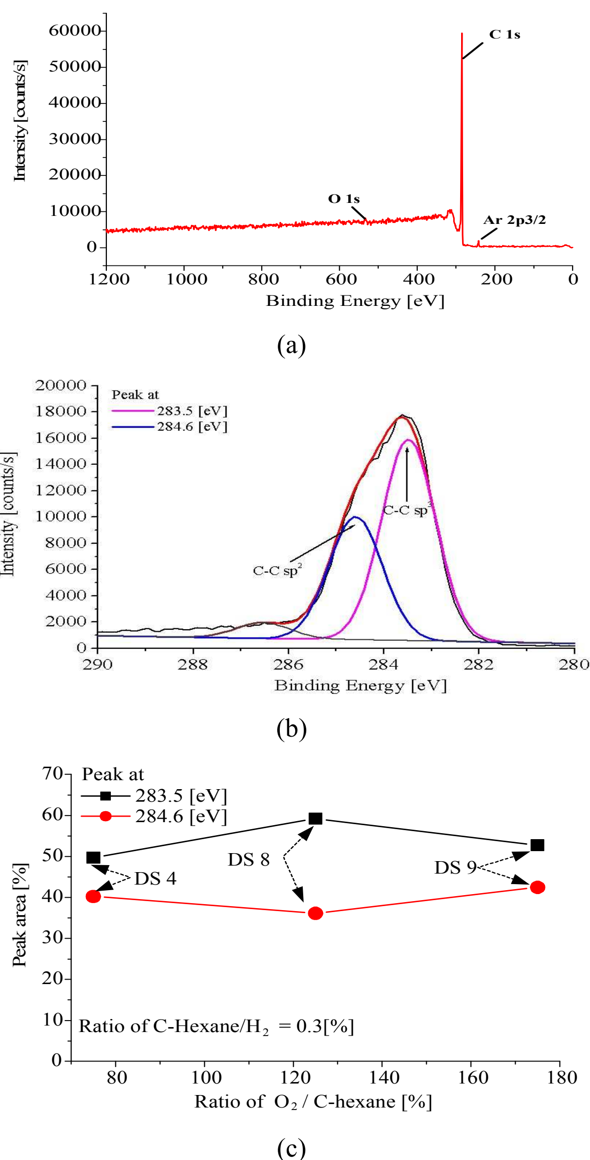

Fig. 5. XPS results according to the ratio of gas mixture: (a) Survey scan spectra; (b) C (1s) spectra and the result of curve fit; (c) Comparison of curve fitting results.

for enhancing the sp^3 chemical bond and deactivating the sp^2 chemical bond simulataneously.

Fig. 5 shows the result of XPS measurement according to the ratio of oxygen to c-hexane amounts. In Fig. 5(a), some peaks correspond to O(1s), C(1s), and Ar(2p 3/2). Ar(2p 3/2) peak exists by Ar bombardment in the etching process. After confirming all peaks by survey scan, the narrow scan was carried out as in Fig. 5(b). Peak areas in Fig. 5(c) were calculated by a curve fitting method using gaussian functions as presented in Fig. 5(b). Contribution of diamond and graphitic components in the binding energy of C(1s) spectra corresponds to 283.5 eV and 284.6 eV, respectively[35]. The peak area of diamond components in the case of the DS8 sample is about 58 %, even though that of graphite is about 35 %. These results agree well with the results in Fig. 4(b).

3.2 Analysis of OES measurement on effects of oxygen and c-hexane contents

The effects of c-hexane and oxygen amounts were discussed with the results of OES measurement. The measurement was carried out 4 times continuously. Emissions of H_α, H_β, and H_γ from hydrogen atom, and CH radicals in the wavelength of 200~800 nm were showed in Fig. 6, which is the same experimental conditions of the DS1 sample. CH (B-X, 388.9 nm) emission is attributed to the transition between the upper vibrational level of B (v'=0) and the lower level of X (v''=0). And the intensity of H_γ is relatively weak in comparison with H_α and H_β. Thus, it was not considered in this work.

Fig. 7 shows the variation of emission intensities on H_α, H_β, CH (B-X), and electron temperature by changing the c-hexane amounts in hydrogen without oxygen. CH (B-X) intensity decreased by increasing c-hexane amounts as shown in Fig. 7(a) and 7(b). The ratio of the maximum

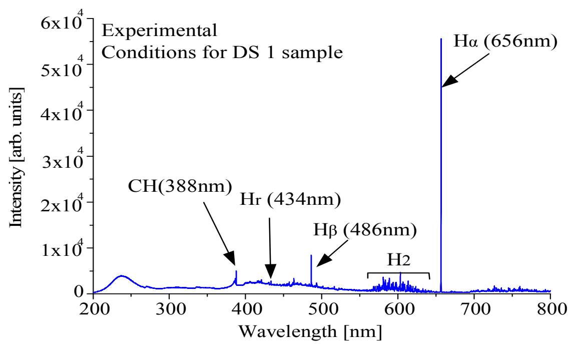

Fig. 6. Emissions in the wavelength of 200~800 nm.

intensity of CH (B-X) emission was at 0.3 % c-hexane to hydrogen. The decrease intendancy of CH (B-X) emission might be caused by the increase of the recombination reaction between CH species and the previously dissociated species such as C_2H_4, C_2H_6, C_xH_y (x, y =1, 2, 3,…), etc.

Antother plausible reason is that the electron collision probability with CH chemical species might be decreased by the increase of the electron collision with other chemical species. Also, the presence of relatively weak CH(B-X) emission at 0 % c-hexane was caused by the residual hydrocarbons from the previous experiment. It does not considered in this work.

From Fig. 7(c) and (d), the electron collision probability with hydrogen atoms decreased as well due to the decrease of both intensities of H_α and H_β. It is ascribed that the generation rate of hydrogen atom from c-hexane by the electron collision reaction does not improved even though c-hexane amounts increased. On the other hand, the recombination reaction between hydrogen atoms and intermediated chemical species from c-hexane might have taken place. This affects the decrease of H_α and H_β intensities eventually. This tendency is similar to the result by S. J. Harris and A. M. Weiner [36]. They found that the concentration of hydrogen atom increased at low CH_4 concentration in comparison with high CH_4 concentrations.

In addition, the electron temperature was not largely changed near 5,000 K as shown in Fig. 7(e).

Consequently, the new chemical reaction between hydrogen atoms and intermediated chemical species from c-hexane was enhanced to generate new chemical species and refrained to the generation both CH species and hydrogen atom at the above 0.3 % c-hexane to hydrogen.

Unfortunatly, the newly generated species could not detect in this measurement system, because those species do not emit lights.

Fig. 8 is to investigate the effects of oxygen amounts under the fixed ratio of 0.3% c-hexane in hydrogen. By increasing oxygen amounts, emission intensities of CH (B-X), H_α, and H_β decreased. Specifically, the emission intensity of the CH (B-X) largely decreased from 0 to 50 % in Fig. 8(a). It might be caused that the generation of new chemical species were formed by the reaction between CH species and oxygen atoms or molecules. Thereafter it suppressed the new generation of CH species from the dissociation of c-hexane.

Another reason is that the electron is easily collied with

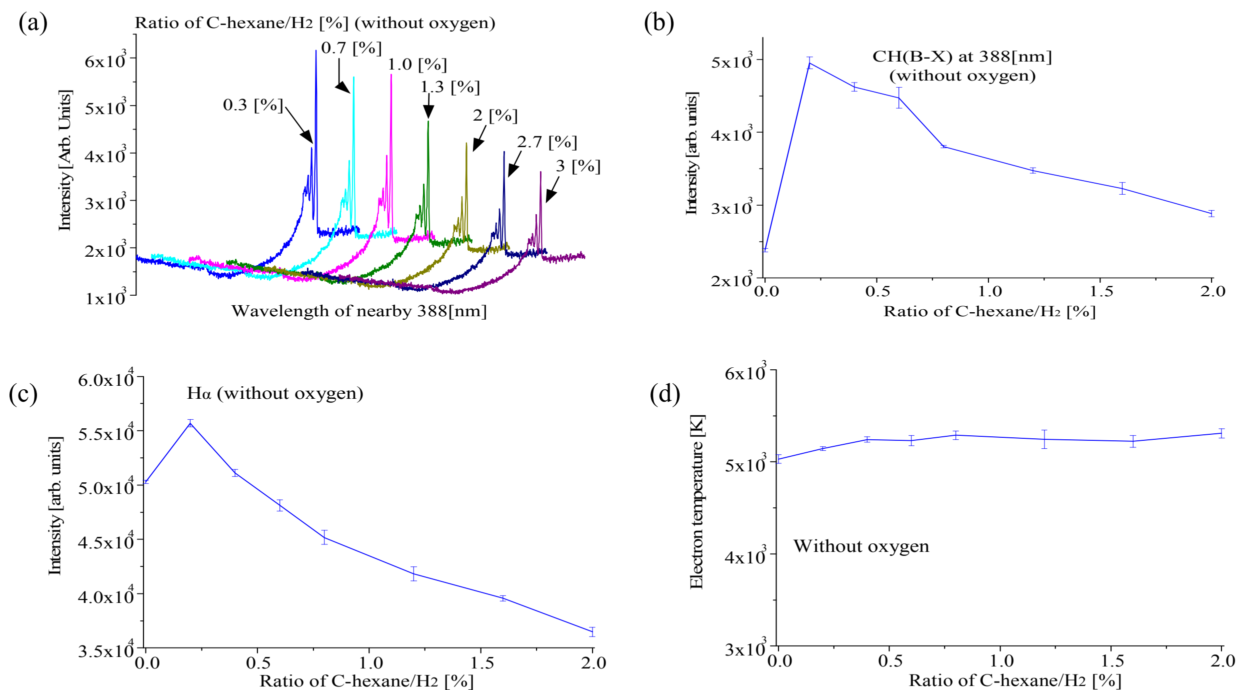

Fig. 7. Variain of emission intensity according to c-hexane amounts without oxygen: (a) CH (B-X); (b) CH (B-X) intensity; (c) H_α; (d) Variation of electron temperature.

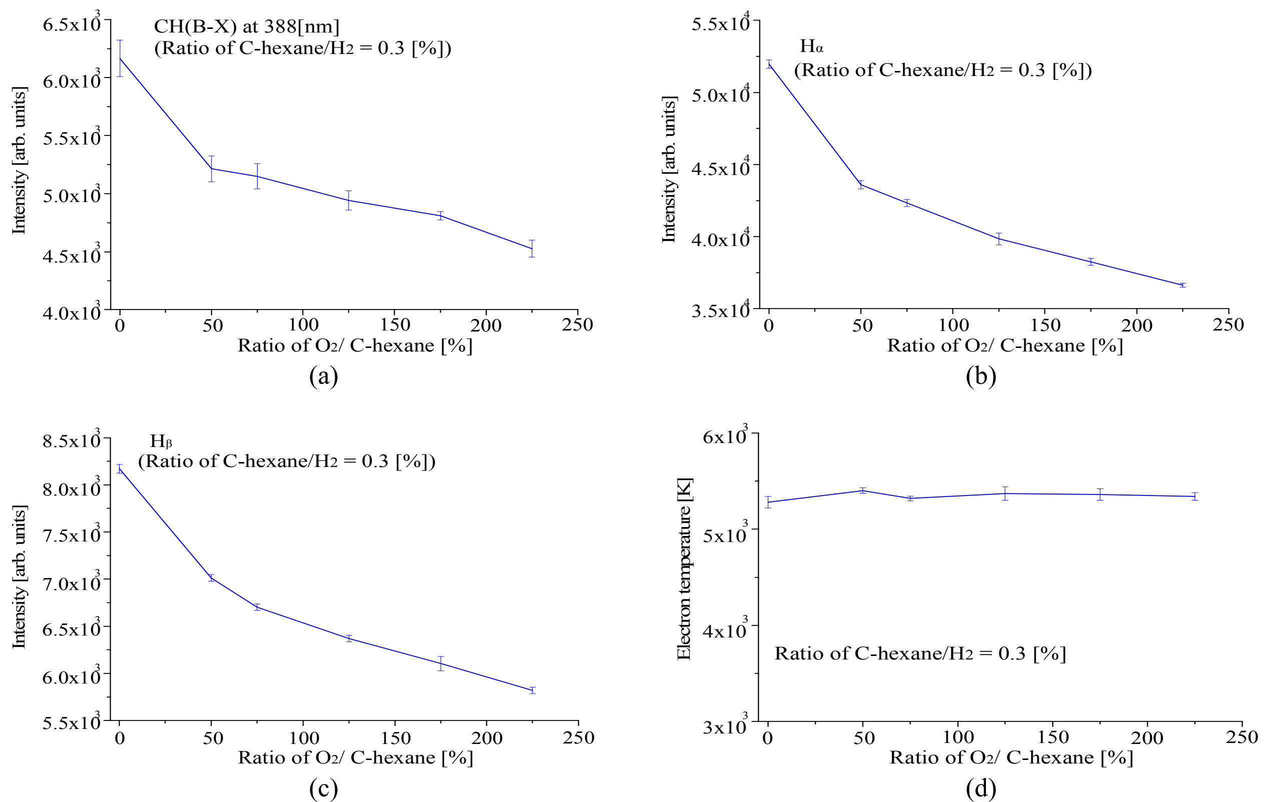

Fig. 8. Variation of emission intensity according to oxygen amounts to c-hexane: (a) CH(B-X); (b) H_α; (c) H_β; (d) Variation of the electron temperature.

oxygen because of the electrical negative gas of oxygen. Oxygen affects the decrease of the excitation possiblity of CH species by decreaing the electron density. Furthermore, the decrease of emissions from hydrogen atoms might be affected by the new generation of chemical species such as OH and other species as shown in Figs. 8(b) and (c). In the case of the electron temperature, it was not largely changed by 5,200 K.

From these results, oxygen plays a role in deactivating the electronic excitation of hydrogen atom and CH species through the electron collision reaction, and generate a new chemical species as well. However, some amounts of oxygen is necessary to synthesize the diamond films as discussed in Figs. 4 and 5.

In comparison with the results in Figs. 4 and 5, the optimum experimental conditions for the synthesis of the high quality polycrystalline diamond films could not easily identified by the analysis of emission intensities of CH (B-X), H_α, and H_β. Moreover, it should be considered that the high quality diamond film did not acquire even though the hign concentration of CH species. Therefore, the analysis of OES measurement should be compared with the experimental conditions of synthesized diamond films.

Based on these results, the optimum oxygen ratio to c-hexane is confirmed at 125 %, which corresponds 0.4% oxygen amounts to hydrogen in this low pressure MWPCVD process.

Moreover, intensities of CH (B-X), H_α, and H_β are about 5×10^3, 4×10^4, and 6.3×10^3. The corresponding intensity ratio of CH (B-X) and H_β related to that of H_α are 12.5 % and 15.75 %, respectively.

4. Conclusion

In this work, the optimum synthesis conditions of polycrystalline diamond films investigates according to the change of gas mixtures. In addition, analytical results of OES measurement is compared with the experimental results.

(1) The effective control of oxygen amounts is important for the synthesis of the high quality polycrystalline diamond films with c-hexane in this low pressure MWPCVD process. The best oxygen ratio to c-hexane was reached at 125 %, which corresponds 0.4% oxygen ratio to hydrogen.

(2) Moreover, the electron temperature was not largely changed as much of 5,000 K ~ 5,200 K according to the change of oxygen and c-hexane amounts. Specifically, the ratio of intensity of CH (B-X) and H_β related to that of H_α on the optimum synthesis conditions are 12.5 % and 15.75 %, respectively.

Acknowledgements

This work was supported by Kyungnam University Foundation Grant No. 20090028.

References

[1] B. V. Spitsyn, L. L. Bouilov, and B. V. Derjaguin, J. Crystal Grow. 52 (1981) 219.
[2] Shr-Ming Huang, Franklin Chau-Nan Hong, Surface and Coatings Technology 200 (2006) 3151.
[3] W.D. Fan, K. Jagannadham, B.C. Goral, Surface and Coatings Technology 81 (1996) 172.
[4] O.A. Williams, Diamond and Related Materials 20 (2011) 621.
[5] A. Deachana, D. Boonyawan, B. Yodsombat, Surface and Coatings Technology 203 (2009) 2743.
[6] P. Ayala, R. Arenal, M. Rümmeli, A. Rubio, T. Pichler, Carbon 48 (2010) 575.
[7] Menghe Miao, Carbon 49 (2011) 3755.
[8] Yasar Gurbuz, Weng Poo Kang, Jimmy L. Davidson, David V. Kerns, and Q. Zhou, IEEE Trans. Power Electronics 20 (2005) 1.
[9] R. Kalish, Diamond and Related Materials 10 (2001) 1749.
[10] Young Yun, Tetsuro Maki, and Takeshi Kobayashi, J. Appl. Phys. 82 (1997) 3422.
[11] Sunwoo Lee, SangYeob Na, J. Electrical Engineering & Technology 6 (2011) 280.
[12] Qingwen Li, Hao Yan, Jin Zhang, Zhongfan Liu, Carbon 42 (2004) 829.
[13] X.J. Hu, J.S. Ye, H.J. Liu, H. Hu, X.H. Chen, Diamond and Related Materials 20 (2011) 246.
[14] C.J. Tang, A. J. S. Fernandes, F. Costa, J. L. Pinto, Vacuum 85 (2011) 1130.
[15] D. Saito, H. Isshiki, T. Kimira, Diamond and Related Materials 18 (2009) 56.
[16] D.A. Tucker, D.-K. Seo, M.-H. Whangbo, F.R. Sivazlian, B.R. Stoner, S.P. Bozeman, A.T. Sowers, R.J. Nemanich, J.T. Glass, Surface Science 334 (1995) 179.
[17] Y. Liao, C.H. Li, Z.Y. Ye, C. Chang, G.Z. Wang, R.C. Fang, Diamond and Related Materials 9 (2000) 1716.
[18] Duosheng Li, Dunwen Zuo, Wenzhung Lu, Rongfa Chen, Bingkun Xiang, Min Wang, Solid State Ionics 179 (2008) 1263.
[19] E Cappelli, S Orlando, G Mattei, A Armigliato, Surface and Coatings Technology, 180-181 (2004) 184.
[20] H. Inaba, S. Fujimaki, K. Furusawa, S. Todoroki, Surface and Coatings Tech. 193 (2005) 277.
[21] S Gupta, G Morell, R.S Katiyar, D.R Gilbert, R.K Singh, Diamond and Related Materials 8 (1999) 185.
[22] Toshiki Tsubota, Shintaro Ida, Naoki Okada, Masanori Nagata, Yasumichi Matsumoto, Nobumitsu Yatsushiro, Surface and Coatings Technology 169–170 (2003) 262.
[23] F. J. Kampas, J. Appl. Phys. 54 (1983) 2276.
[24] E. Staryga, G. W. Bak, K. Fabisiak, L. Klimek, A. Rylski, A. Olborska, M. Kozanecki, J. Grabarczyk, Vacuum 85 (2010) 518
[25] A. Grigonis, V. Sablinskas, M. Silinskas, D. Tribandis, Vacuum 75 (2004) 261.
[26] S.R.J. Pearce, S.J. Henley, F. Claeyssens, P.W. May, K.R. Hallam, J.A. Smith, K.N. Rosser, Diamond and Related Materials 13 (2004) 661.
[27] L. Yang, P.W. May, L. Yin, J.A. Smith, K.N. Rosser, Diamond and Related Materials 16 (2007) 725.
[28] R.T Rozbicki, V.K Sarin, Thin Solid Films 332 (1998) 87.
[29] Marcus Asmann, Joachim Heberlein, Emil Pfender, Diamond and Related Materials 8 (1999) 1.
[30] A. Qayyum, R. Ahmad, S.A. Ghauri, A. Waheed, M. Zakaullah Vacuum 80 (2006) 574.
[31] T. Sharda, T.Soga, T. Jimbo, and M.Umeno, Diamond and Related Materials 9 (2000) 1331.
[32] Sathyaharish Jeedigunta, Zhenqing Xu, Makoto Hirai, Priscila Spagnol, Ashok Kumar, Diamond and Related Materials 17 (2008) 1994.
[33] X. M. Meng et al., Int. J. Refractory Metals and Hard Materials 26 (2008) 485.
[34] Y. S. Li, Y. Tang, Q. Yang, S. Shimada, K. Y. Lee, A. Hirose, Int. J. Refractory Metals and Hard Materials 26 (2008) 465.
[35] A. Bendavid, P.J. Martin, L. Randeniya, M.S. Amin, Diamond and Related Materials 18 (2009) 66.
[36] Stephen J. Harris and Anita M. Weiner, J. Appl. Phys. 67 (1990) 6520.

Sang-Bo Han received the B.E. and M.E Degrees in Electrical Engineering from the Kyungnam University, Korea, in 1998 and 2000, respectively, and the Ph.D. Degree in Electronic Engineering from the University of Tokyo, Japan, in 2004. He is currently an Assistant Professor in the Department of Electrical Engineering at the Kyungnam University. His research interests are industrial applications of carbon films in PECVD process, the control of plasma process, and the application of non-thermal plasma and electrostatics.

Dr. Han is a Member of the Korean Institue of Electrical Engineers, Korean Institute of Illuminating and Electrical Installation Engineers, and Institute of Electrostatics in Japan.